Fuzzy-Cuts: A Knowledge-Driven Graph-Based Method for Medical Image Segmentation

D.R. Chittajallu G. Brunner U. Kurkure R.P. Yalamanchili I.A. Kakadiaris

Computational Biomedicine Lab, Depts. of Computer Science, Elec. & Comp. Engineering, and Biomedical Engineering, Univ. of Houston, Houston, TX, USA

{drchittajallu,gbrunner,ukurkure,rpyalamanchili2,ioannisk}@uh.edu

Abstract

Image segmentation is, in general, an ill-posed problem and additional constraints need to be imposed in order to achieve the desired result. Particularly in the field of medical image segmentation, a significant amount of prior knowledge is available that can be used to constrain the solution space of the segmentation problem. However, most of this prior knowledge is, in general, vague or imprecise in nature, which makes it very difficult to model. This is the problem that is addressed in this paper. Specifically, in this paper, we present Fuzzy-Cuts, a novel, knowledge-driven, graph-based method for medical image segmentation. We cast the problem of image segmentation as the Maximum A Posteriori (MAP) estimation of a Markov Random Field (MRF) which, in essence, is equivalent to the minimization of the corresponding Gibbs energy function. Considering the inherent imprecision that is common in the a priori description of objects in medical images, we propose a fuzzy theoretic model to incorporate knowledge-driven constraints into the MAP-MRF formulation. In particular, we focus on prior information about the object's location, appearance and spatial connectivity to a known seed region inside the object. To that end, we introduce fuzzy connectivity and fuzzy location priors that are used in combination to define the first-order clique potential of the Gibbs energy function. In our experiments, we demonstrate the application of the proposed method to the challenging problem of heart segmentation in non-contrast computed tomography (CT) data.

1. Introduction

Image segmentation is at the core of higher level analysis of medical images. It constitutes an integral part of a variety of applications including study of anatomical structures, quantification of tissue volumes, localization of pathologies, computer-aided diagnosis, and image-guided surgery. However, image segmentation is, in general, an ill-posed problem and additional constraints need to be imposed in order to achieve the desired solution. The commonly used constraints include the traditional regularization constraints and those derived from prior knowledge about the objects being segmented (e.g., shape, appearance, location). A variety of approaches have been proposed both for image segmentation in general [13] and for medical image segmentation in particular [16]. However, the energy minimization formulation of the segmentation problem, or the equivalent probabilistic formulation of Maximum a Posteriori (MAP) probability estimation, tend to be more suitable for taking into account the need for the incorporation of various constraints into the problem. Particularly in the field of medical image segmentation, a significant amount of prior knowledge is usually available and can be exploited to constrain the solution space of the segmentation problem. However, most prior knowledge available in the field of medical image segmentation is vague or imprecise in nature, which makes it very difficult to model. Moreover, it is an even greater challenge to unify the information from such a wide variety of sources into a single framework. This is precisely the problem that is addressed in this paper.

In this paper, we present *Fuzzy-Cuts*, a novel, knowledge-driven, graph-based method for medical image segmentation. Specifically, we cast the problem of image segmentation as the MAP estimation of a Markov Random Field (MRF), the solution to which can be obtained by minimizing the corresponding Gibbs energy function that is essentially a sum of clique potentials. For the purposes of this paper, we only consider the first- and second-order clique potentials. We then use graph-cuts to minimize the Gibbs energy [7, 9]. Our main contribution is the definition of the first- and second-order clique potentials. We derive the first-order clique potential using an elegant fuzzy set theoretic framework that attempts to model the inherent fuzziness found in the *a priori* description of objects in medical

978-1-4244-3991-1/09/$25.00 ©2009 IEEE

images. Specifically, we focus on the incorporation of the following two types of prior knowledge:

- **Appearance and spatial connectivity prior:** While segmenting organs in medical images, we know that each organ is composed of a set of tissues which in turn have a characteristic appearance or texture. This prior knowledge about the texture or appearance of the tissues composing the organs can be used to improve the segmentation. However, since it is possible that two different organs can be composed of the same tissue, using only appearance information will result in the erroneous segmentation of both the organs as a single object. Hence, both appearance and spatial connectivity to the seed region of the object are equally important in achieving a good segmentation result.

- **Location prior:** Since the acquisition process of medical images is standardized, prior knowledge about the anatomical location of the organs can be used to our advantage while segmenting organs in medical images. The location of organs is commonly specified relative to other neighboring organs.

We model the appearance and spatial connectivity prior using fuzzy connectedness [19] and we use the framework of fuzzy spatial relationships [1, 5] to model the location prior. We define the second-order clique potentials using a generalized Potts Interaction model. Specifically, we extend the definition of Boykov *et al.* [2] to the multi-feature scenario.

This paper is organized as follows: In Section 2, we describe in detail the theoretical foundation of our Fuzzy-Cuts algorithm. In Section 3, we demonstrate the application of Fuzzy-Cuts to the challenging problem of heart segmentation in non-contrast CT data and present our segmentation results. Finally, in Section 4 we present our conclusions.

2. Fuzzy-Cuts

In this section, we present the theory behind Fuzzy-Cuts. Specifically, we begin by formulating the segmentation problem as the minimization of a Gibbs energy function with first- and second-order cliques in Section 2.1. We then present our definitions for the first- and second-order clique potentials in Sections 2.2 and 2.3, respectively. Finally, in Section 2.4 we discuss the minimization of the segmentation energy using graph-cuts. A brief outline of the steps involved in our segmentation algorithm *Fuzzy-Cuts* is given below:

Algorithm *Fuzzy-Cuts*

1. Compute fuzzy connectivity prior (Sec. 2.2.1).
2. Compute fuzzy location prior (Sec. 2.2.2).
3. Compute first-order clique potentials using fuzzy connectivity and location priors (Sec. 2.2).
4. Compute second-order clique potentials using a generalized Potts model (Sec. 2.3).
5. Minimize Gibbs energy using graph-cuts (Sec. 2.4).

2.1. Formulation of the segmentation problem

The image segmentation problem is a labeling problem. More formally, consider an image I and let $P = \{1, 2, ..., M\}$ be the set of M pixels (or voxels) of the image and let $L = \{l_1, ..., l_H\}$ be the set of H labels assigned to the H objects to be segmented. The goal of image segmentation is to find a mapping $F : P \rightarrow L$ that is optimal in some sense. The Markov random field (MRF) theory provides an elegant mathematical framework for solving this problem [12]. Using the MRF framework, we define the labeling $F = \{F_1, ..., F_M\}$ as a field of random variables defined on the set of pixels P, wherein each random variable F_i is associated with a pixel $i \in P$ and takes on a value f_i from the set of labels L. Any possible assignment $f = \{f_1, ..., f_M\}$ of labels to the random variables is called a configuration of F, and is essentially a realization of the field. Note that every configuration f defines a segmentation and we denote the set of all possible configurations as $\mathbb{F}$. We also define a neighborhood system $N = \{N_i \mid \forall i \in P\}$ for the set of pixels P, where N_i is the set of all neighbors of the pixel $i \in P$. For example, this can be a 4- or 8-neighborhood system for 2D images and a 6- or 26-neighborhood system for 3D images. Now F qualifies as an MRF with respect to the neighborhood system N if and only if it satisfies the following two properties:

$$\begin{aligned} Positivity: &\quad \Pr(f) > 0, \forall f \in \mathbb{F} \\ Markovianity: &\quad \Pr(f_i \mid f_{P-\{i\}}) = \Pr(f_i \mid f_{N_i}), \forall i \in P \end{aligned}$$

The Markovian property dictates that the label f_i assigned to a pixel i depends only on the labels f_{N_i} assigned to its neighboring pixels N_i. This condition is generally true for medical images: the statistics of a pixel in a medical image is related to the statistics of the pixels in a small local neighborhood around it [6]. Now that we have an MRF, we need to find a way to model the probability $\Pr(f \mid D)$ of a particular labeling configuration f given the observed image data D. The Hammersley-Clifford theorem [8] provides an elegant solution to this problem. According to this theorem an MRF is equivalent to a Gibbs random field (GRF) which includes an interesting and beneficial property: A random field F qualifies as a Gibbs random field if it obeys the Gibbs distribution that can be specified as follows:

$$\Pr(f) = Z^{-1} \cdot \exp\left(-E(f)\right), \tag{1}$$

where Z is a normalizing constant and $E(f)$ is the Gibbs energy function. The Gibbs energy function

$$E(f) = \sum_{c \in C} V_c(f) \tag{2}$$

is essentially a sum of clique potentials $V_c(f)$ over the set of all possible cliques, C. A clique c, in our case, can be defined as a subset of the set P of pixels such that each member of the set is a neighbor of all the other members. The value of $V_c(f)$ depends on the local configuration of the clique c. The number of pixels in a clique defines the order of the clique and the corresponding clique potential. For the purposes of this paper, we only consider first- and second-order cliques. In this case, the Gibbs energy can be expressed as follows:

$$E(f) = \sum_{i \in P} V_i(f_i) + \sum_{i \in P} \sum_{j \in N_i} V_{ij}(f_i, f_j), \qquad (3)$$

where V_i and V_{ij} are the first- and second-order clique potential functions, respectively. Now that we have found a convenient way to model $\Pr(f \mid D)$, the optimal or MAP labeling f^* of the MRF can be defined as

$$f^* = \arg\max_{f \in \mathbb{F}} \Pr(f \mid D) \qquad (4)$$

which is equivalent to minimizing the Gibbs energy function $E(f \mid D)$ conditioned over the observed data D as shown below:

$$E(f \mid D) = \sum_{i \in P} V_i(f_i \mid D) + \sum_{i \in P} \sum_{j \in N_i} V_{ij}(f_i, f_j \mid D). \qquad (5)$$

We refer to Eq. 5 as the segmentation energy. In order to achieve the desired segmentation, our next challenges are to define the first- and second-order clique potentials V_i and V_{ij}, and then to find an efficient way to minimize the segmentation energy $E(f \mid D)$. Section 2.4 discusses how to minimize the energy function using graph-cuts. Sections 2.2 and 2.3 present our definitions of the first- and second-order clique potentials.

2.2. Definition of first-order clique potential

The first-order clique potential $V_i(f_i \mid D)$ in Eq. 5 measures the cost or penalty incurred in assigning a label f_i to the pixel i given the data D. In probabilistic terms, it measures the degree to which the event of assigning a label f_i to pixel i disagrees with prior knowledge about the objects being segmented. Owing to the inherent imprecision or fuzziness that is common in the description of objects in medical images, we use a fuzzy set theoretic framework to unify any prior knowledge about the objects being segmented. Specifically, in this paper, we consider prior knowledge about the object's location, appearance and spatial connectivity to a known seed region of the object. We define the first-order clique potential as a fuzzy set defined on the image space S as:

$$V_i(f_i \mid D) = \hat{c}\left(t\left(\mu_\chi^{O_z}(i), \mu_\lambda^{O_z}(i)\right)\right), \qquad (6)$$

where $\mu_\chi^{O_z}(i) : S \rightarrow [0,1]$ and $\mu_\lambda^{O_z}(i) : S \rightarrow [0,1]$ are fuzzy sets defined on the image space S, t is the t-norm operator representing fuzzy conjunction of two fuzzy sets and $\hat{c}$ is the fuzzy complement operator. The term $\mu_\lambda^{O_z}(i)$ models prior information about the location of the object O_z in the image space, where O_z is an object with label l_z and, $f_i = l_z$ given a particular segmentation f. The term $\mu_\chi^{O_z}(i)$ models prior information about the appearance and spatial connectivity to a known seed region of the object O_z. Further details about $\mu_\chi^{O_z}$ and $\mu_\lambda^{O_z}$ are discussed in Sections 2.2.1 and 2.2.2, respectively.

2.2.1 Fuzzy connectivity prior

We use fuzzy connectedness, originally introduced by Udupa *et al.* [19], to model $\mu_\chi^{O_z}(i)$ in Eq. 6, representing prior knowledge about the appearance and spatial connectivity to a seed region of the object O_z. Fuzzy connectedness allows us to realize a fuzzy theoretic model corresponding to the following notion [17]:

> *"If two regions have about the same appearance and if they are spatially connected to each other in the image space then they most likely belong to the same object."*

For the purposes of this paper, given a seed region of the object, we can use fuzzy connectedness to compute a fuzzy connected component that assigns to each pixel in the image space a membership value that represents the degree to which the pixel is connected to the seed region. The relation of "connectedness" is a fuzzy relation (as opposed to a crisp binary relation) that is a function of both similarity in appearance and spatial connectivity to the seed region of the object. In other words, if a pixel is spatially connected to the seed region through a path of pixels where each pixel has an appearance close to that of the seed region, then it is assigned a high membership value. Specifically, let R be the seed region of the object O_z, then using fuzzy connectedness we define $\mu_\chi^{O_z}(i)$ as a fuzzy set representing a fuzzy connected component of the object O_z as shown below:

$$\mu_\chi^{O_z}(i) = \max_{p_{Ri} \in P_{Ri}} \left\{ \min_{1 \leqslant j < |p_{Ri}|} \left[\psi^{O_z}(j, j+1)\right] \right\}, \qquad (7)$$

where p_{Ri} is any path of pixels connecting R to pixel i, P_{Ri} is the set of all possible paths connecting R to i, and $\psi^{O_z}(j, j+1)$ is a local fuzzy relation representing the affinity or "hanging togetherness" between two consecutive pixels j and $j+1$ on the path p_{Ri} consisting of $|p_{Ri}|$ pixels. According to Eq. 7, the degree of connectedness of a pixel i to the object O_z is equal to the strength of the strongest path connecting the seed region R to the pixel i where the strength of a particular path is equal to the weakest affinity between successive pairs of pixels along the path. The key

to good performance from fuzzy connectedness depends heavily on an appropriate definition of local fuzzy affinity relation $\psi^{O_z}(p,q)$ representing the degree to which two spatially adjacent pixels p and q in the image space belong to the same object. A generalized form of the fuzzy affinity relation proposed by Udupa *et al.* [19] is given by:

$$\psi^{O_z}(p,q) = \begin{cases} \mu_\nu^{O_z}(p,q) \cdot \mu_\alpha^{O_z}(p,q) & \text{if } p \neq q \\ 1 & otherwise \end{cases} \quad (8)$$

where $\mu_\nu^{O_z}(p,q)$ is a simple adjacency test on the pixels p and q which is equal to 1 if the two pixels are spatially adjacent in the image space and zero otherwise. The fuzzy function $\mu_\alpha^{O_z}(p,q)$ measures the degree to which the two pixels p and q belong to the same object in terms of appearance, taking their intensities and local image properties into account. A variety of definitions of the fuzzy affinity relation are available in the literature [19, 15], most of them differing in the way the function $\mu_\alpha^{O_z}(p,q)$ is designed, and each of them has its own advantages. Any definition of the fuzzy affinity relation that is suitable to the specific application at hand can be straightforwardly plugged into our framework. For the purposes of this paper, we extend the definition of Udupa *et al.* [19] to a generalized multi-feature version given by:

$$\begin{aligned} \mu_\alpha^{O_z}(p,q) &= w_1 \cdot \Pr\left(x = \frac{(D_p + D_q)}{2}; \theta_1^{O_z}\right) \\ &\quad + w_2 \cdot \Pr\left(x = |D_p - D_q|; \theta_2^{O_z}\right), \end{aligned} \quad (9)$$

where D_p and D_q are the feature vectors of pixels p and q, respectively. The term $\Pr(x; \theta_1^{O_z})$ is a probability density function (pdf) of the feature values of the object O_z, and $\theta_1^{O_z}$ is the vector of parameters governing this density function. The term $\Pr(x; \theta_2^{O_z})$ is a probability density function of the difference in feature values of neighboring pixels (feature homogeneity) in the object O_z, and $\theta_2^{O_z}$ is the vector of parameters governing this density function. The weights w_1 and w_2 provide control over the amount of importance given to individual terms in Eq. 9 and we assume that $w_1 + w_2 = 1$. Specifically, the first term in Eq. 9 is the feature-affinity term that measures the degree to which the mean feature vector of pixels p and q belongs to the the object O_z given a pdf of the feature values of the pixels in the object. The second term in Eq. 9 is the homogeneity term that measures the degree to which the feature homogeneity between the pixels p and q agrees with the homogeneity with that of the object O_z given a pdf representing the feature homogeneity of neighboring pixels in the object O_z.

2.2.2 Fuzzy location prior

In this section, we describe various fuzzy approaches that can be employed to define the spatial fuzzy set $\mu_\lambda^{O_z}(i)$ (see Eq. 6) representing prior information about the location of the object O_z in the image space. Anatomical description of the location of organs is often specified in terms of their spatial relationship with other neighboring organs. Additionally, these descriptions are vaguely specified in natural language which is far from a pixel-level description. As a typical example, consider the anatomical location of the heart which is usually described as follows:

- the heart is located "within" the thoracic cavity,
- the heart is located "between" the lungs, and
- the heart is located "superior to" the diaphragm.

However, notice that there is an inherent structure in this description that can be exploited. The location of the organ of interest (heart) is specified as a conjunctive combination of its spatial relationship with each neighboring organ. Based on these inferences, we propose to model $\mu_\lambda^{O_z}(i)$ as a fuzzy conjunction of the spatial relationship of object of label f_i with each of its neighboring objects where each one of these relationships is in turn a fuzzy spatial set. More formally, we define $\mu_\lambda^{O_z}(i)$ to be a fuzzy set defined on the image space S as follows:

$$\mu_\lambda^{O_z}(i) = t\left(..., \mu_{NO_k}^{O_z}(i), ...\right); \quad k = \{1, 2..., T\} \quad (10)$$

where T is the total number of neighboring objects involved in the description of the location of the object O_z, $\mu_{NO_k}^{O_z}(i)$ is a spatial fuzzy set representing the spatial relationship of the object O_z with the k^{th} neighboring object, and t is the t-norm operator representing a fuzzy conjunction of all the fuzzy sets involved. A variety of ways to define different kinds of fuzzy spatial relationships between objects (e.g., "inside", "outside", "left of", "right of", "above", "below"). are available in the literature, a summary of which can be found in [1]. Note that the proposed model is applicable assuming that we have either a crisp or fuzzy segmentation of the neighboring objects. Alternatively to the proposed model, one can also perform atlas registration and use a probabilistic atlas [14] to represent $\mu_\lambda^{O_z}(i)$.

2.3. Definition of second-order clique potential

The second-order clique potential function $V_2(f_i, f_j \mid D)$ in Eq. 5 measures the cost or penalty incurred in jointly assigning a label f_i to the pixel i and a label f_j to the pixel $j \in N_i$ given the data D. We model this as a piecewise constant prior using a Generalized Potts Interaction model [3] as shown below:

$$\begin{aligned} V_{ij}(f_i, f_j \mid D) &= K(i,j \mid D) \cdot (1 - \delta(|f_i - f_j|)) \\ &= \begin{cases} K(i,j \mid D) & \text{if } f_i \neq f_j \\ 0 & otherwise \end{cases} \end{aligned} \quad (11)$$

For $K(i,j \mid D)$ we extend the definition of Boykov *et al.* [2, 4] to a multi-feature version which we express as follows:

$$K(i,j \mid D) = \exp\left(-(D_i - D_j)^T \Sigma_k^{-1} (D_i - D_j)\right), \quad (12)$$

where D_i and D_j are the feature vectors of pixels i and j, respectively. The term Σ_k is the covariance matrix which can represent the amount of variability allowed between the feature vector values of two neighboring pixels within an object. This function assigns a higher penalty if two neighboring pixels with similar feature vector values are assigned different labels. Specifically, if the dissimilarity between the two pixels i and j in the feature space is within the amount of variability allowed by Σ_k then the event of assigning different labels to them is highly penalized.

2.4. Minimizing $E(f \mid D)$ using graph-cuts

Minimizing the energy function $E(f \mid D)$ is a significant part of the challenge in solving an image segmentation problem. Graph-cuts provides an efficient way to optimize such energy functions [10] owing to certain constraints. Particulary in the case of a binary segmentation problem, where $L = \{0,1\}$, graph-cuts provides us with a globally optimal solution provided that V_{ij} is a sub-modular function (i.e., $V_{ij}(0,0) + V_{ij}(1,1) \leq V_{ij}(0,1) + V_{ij}(1,0)$) [10]. The more general case of multiple-object segmentation, where $H > 2$, with a segmentation energy based on the generalized Potts model can be solved by formulating it as a multi-way cut problem [3], which unfortunately has been proven to be NP-Hard. However the $\alpha - expansion$ algorithm proposed by Boykov *et al.* [3] has been proven to find good approximate solutions to this problem.

In this section, we present a brief overview of the graph construction procedure for the general case of multiple-object segmentation that can be cast as an optimal multi-way cut problem. The optimal multi-way cut problem is essentially a generalization of the binary, two-terminal, s-t minimum cut problem to the multiple-label scenario. Consider a directed and edge-weighted graph $\mathbb{G} = \langle \mathcal{V}, \mathcal{E} \rangle$ where $\mathcal{V}$ is the set of vertices or nodes and $\mathcal{E}$ is the set of directed edges with non-negative weights. The set $\mathcal{V}$ contains two types of nodes: p-nodes, denoted $\mathcal{V}_P$, for the set P of pixels (or voxels) in the image space, and l-nodes, denoted $\mathcal{V}_L$, for the set L of labels which are also called terminals. Thus, we have $\mathcal{V} = P \cup L$. Correspondingly, we have two types of edges: n-links, denoted $\mathcal{E}_N$, for edges between p-nodes, and t-links, denoted $\mathcal{E}_L$, for edges connecting p-nodes to l-nodes. The t-links and n-links correspond to first- and second-order cliques of the MRF F discussed in Section 2.1. Two p-nodes are connected by an edge if and only if they are neighboring pixels in the neighborhood system N of the MRF F. Thus, each n-link $\{i,j\} \in \mathcal{E}_N$, where $i,j \in P$, in the graph represents a second-order clique between the corresponding pixels (or sites) of our MRF F and hence is assigned a weight w_{ij} equal to the corresponding second-order clique potential (i.e., $w_{ij} = K(i,j \mid D)$) (see Section 2.1). Similarly, each t-link $\{i,l\} \in \mathcal{E}_L$ in the graph represents a first-order clique of our MRF F corresponding to the pixel (or site) $i \in P$ and label $l \in L$ and hence is assigned a weight w_{il} based on the corresponding first-order clique potential (i.e., $w_{il} = W_i - V_i(l)$, where $W > \max_{l \in L}\{V_i(l)\}$) (see Section 2.1). A multi-way cut is a subset of edges $\mathcal{C} \in \mathcal{E}$ such that all the l-nodes or terminals are completely separated in the induced graph $\mathbb{G}(\mathcal{C}) = \langle \mathcal{V}, \mathcal{E} - \mathcal{C} \rangle$. Additionally, it is required that no proper subset of $\mathcal{C}$ separates the terminals in $\mathbb{G}(\mathcal{C})$. The cost $|\mathcal{C}|$ of the multi-way cut is equal to the sum of its edge weights. The optimal multi-way cut problem corresponds to finding the minimum cost multi-way cut. With the current graph construction it is easy to see that the minimum-cost multi-way cut minimizes the segmentation energy in Eq. 5. A summary of the weights assigned to the different types of edges in the graph $\mathbb{G}$ is depicted in the following table.

Edge	Weight (Cost)	for
$\{i,j\}$	$K(i,j \mid D)$	$\{i,j\} \in N$
$\{i,l\}$	$W_i - V_i(l)$	$i \in P, l \in L$

3. Experiments: Heart Segmentation

In this section, we demonstrate how to apply *Fuzzy-Cuts* to the problem of heart segmentation in non-contrast CT data. Specifically, we applied Fuzzy-Cuts to segment the heart in 2D axial slices taken at the z-level of the origin of aorta. A sample image is shown in Figure 1(a). Notice that this is a binary (foreground-background) segmentation problem: we have only two labels ($L \in \{0,1\}$) where the heart is our foreground object and everything else is considered as background. Also note that we only use one feature per pixel, namely the intensity value of the pixel, and we use a 4-neighborhood system. In Sections 3.1 - 3.5 we discuss the implementation details of each individual step in the *Fuzzy-Cuts* Algorithm. Finally, in Section 3.6 we present the segmentation results obtained and compare them with the results obtained using other methods.

3.1. Computation of the fuzzy connectivity prior

We compute the fuzzy connectivity prior using Eqs. 8 and 9. We use only the feature affinity term in Eq. 9 by setting $w_1 = 1$ and $w_2 = 0$. We use a Gaussian mixture model to model the pdfs of the intensity values of the foreground and background object. Specifically, we model the pdf of the foreground (heart) using a single Gaussian distribution representing the intensities of the blood and muscle tissues

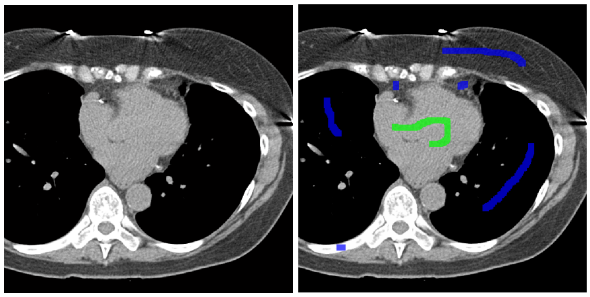

(a) (b)

Figure 1. (a) An axial CT slice taken at the z-level of the origin of aorta. (b) The foreground (green) and background (blue) seed regions interactively specified by the user.

of the heart, and we model the pdf of the background using a mixture of three Gaussian distributions representing the air, fat and bone tissues of the organs neighboring the heart. The parameters of these Gaussian distributions can be derived from seed regions corresponding to each tissue which can be obtained either automatically or interactively. For the purposes of this paper, the parameters of the Gaussian distributions are determined from the user-initialized seed regions in each of the tissues involved. Specifically, the user provides one or more brush strokes for each tissue using an interactive tool. Figure 1(b) depicts the user-initialized seed regions for the foreground and background objects and Figures 4(a) and (b) depict the fuzzy connectivity priors of the foreground and background objects.

3.2. Computation of the fuzzy location prior

According to prior knowledge from anatomy, the location of the heart in Figure 1(a) can be described as follows:

- the heart is located "between" the lungs,
- the heart is located "within" the thoracic cavity, and
- the probability of a pixel belonging to the heart increases as we go towards the center of the cavity between the lungs and inside the inner thoracic cavity.

In order to incorporate this prior knowledge into the segmentation process, we first segment the lungs using simple thresholding and connected component analysis. We then segment the thoracic cavity using a dynamic programming based method [11]. Note that the thoracic cavity encloses the heart and the lungs. We compute a binary mask of the cavity between the lungs and inside the thoracic cavity by excluding the lung masks from the thoracic cavity mask. We refer to this as the heart cavity mask. Figure 2 depicts the binary masks of the left lung, right lung, the thoracic cavity and the heart cavity. We use the binary mask of the thoracic cavity to represent the spatial relation "within" with the thoracic cavity. Note that a binary mask is a crisp set which is a special case of a fuzzy set. We use a simple normalized distance map to represent the prior knowledge that the heart pixels are more likely to be found towards the center of the heart cavity mask. In order to represent the spatial relationship "between" with respect to the lungs, we reduce it to two fuzzy directional relations, one with the left lung and the other with the right lung. Let O_1 and O_2 be the centroids of the left and right lung respectively, and let $\overrightarrow{O_1O_2}$ be the unit vector representing the direction of the vector joining O_1 and O_2. The heart is located in the direction of $\overrightarrow{O_1O_2}$ of the left lung and in direction of $\overrightarrow{O_2O_1}$ of the right lung. We use the fuzzy mathematical morphology based approach proposed by Bloch *et al.* [1] to model these directional relationships. Figure 3 depicts the fuzzy maps of all the spatial relationships discussed above. We compute the fuzzy location prior of the foreground as a fuzzy conjunction (t-norm) of the fuzzy maps of all the spatial relationships. We use the "min" operator as the t-norm operator to compute the fuzzy conjunction and we compute the fuzzy location prior of background as a fuzzy complement of the foreground prior. Figures 4(c) and (d) depict the fuzzy location prior of the foreground and the background objects.

(a) (b) (c) (d)

Figure 2. Binary masks of: (a) left lung, (b) right lung, (c) thoracic cavity, and (d) heart cavity.

(a) (b) (c) (d)

Figure 3. Fuzzy spatial relationships: (a,b) the heart is located "between" the left and the right lung, (c) the heart is located "within" thoracic cavity, and (d) the probability of a pixel belonging to the heart increases as we go towards the center of the heart cavity.

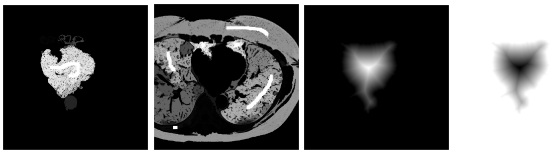

(a) (b) (c) (d)

Figure 4. (a,b) Depiction of the fuzzy connectivity prior for the foreground and background object, respectively. (c,d) Depiction of the fuzzy location prior for the foreground and background object, respectively.

3.3. Computation of first-order clique potentials

We compute the first-order clique potentials as a fuzzy conjunction (t-norm) of the two fuzzy sets representing the fuzzy connectivity prior and the fuzzy location prior as detailed in Eq. 6. Specifically, we use the product as the t-norm operator to compute the fuzzy conjunction. Figures 5(a) and (b) depict the first-order clique potentials for the foreground and the background object.

3.4. Computation of second-order clique potentials

We compute the second-order clique potentials using a generalized Potts model (Section 2.3). Since we consider only one feature value, namely the intensity, we set Σ_k equal to the variance of the difference between intensity values of neighboring pixels within the foreground and background seed regions. Any variability between the intensities beyond Σ_k more likely belongs to the interface between the foreground and the background object and hence receives a high penalty. Since we consider a 4-neighborhood system, we have two kinds of second-order cliques: (1) spatial interactions between neighboring pixels along the x-axis, and (2) spatial interactions between neighboring pixels along the y-axis of the image. Figures 5(c) and (d) depict the potentials of the second-order cliques along the x- and y-directions.

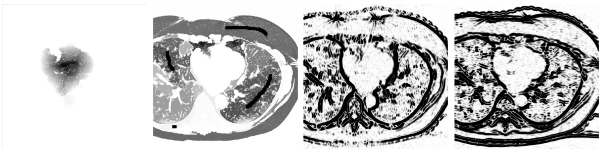

(a) (b) (c) (d)

Figure 5. (a,b) Depiction of the first-order clique potentials for the foreground and background object, respectively. (c,d) Depiction of the second-order clique potentials between pixels along the x- and y-directions, respectively.

3.5. Energy minimization using graph-cuts

After computing all the terms of the Gibbs energy, we construct the graph (Section 2.4). Since the problem under consideration is a binary segmentation problem, optimization using graph-cuts provides a global minimum for our segmentation energy.

3.6. Results and Discussion

Figure 6 depicts the segmentation result of Fuzzy-Cuts in comparison with other approaches. Specifically, we evaluated the performance of Fuzzy-Cuts in the following three scenarios:

(a) **Fuzzy-Cuts with and without fuzzy location prior**
Figures 6(a) and (b) depict a comparison of the segmentation results obtained using Fuzzy-Cuts with and without fuzzy location prior. As is evident from Figure 6(b) that due to the lack of location prior the tissues of the neighboring organs spatially connected to the foreground seed region by a strong fuzzy affinity path were incorrectly labeled as foreground. This suggests that the location prior is equally important in achieving the desired segmentation result.

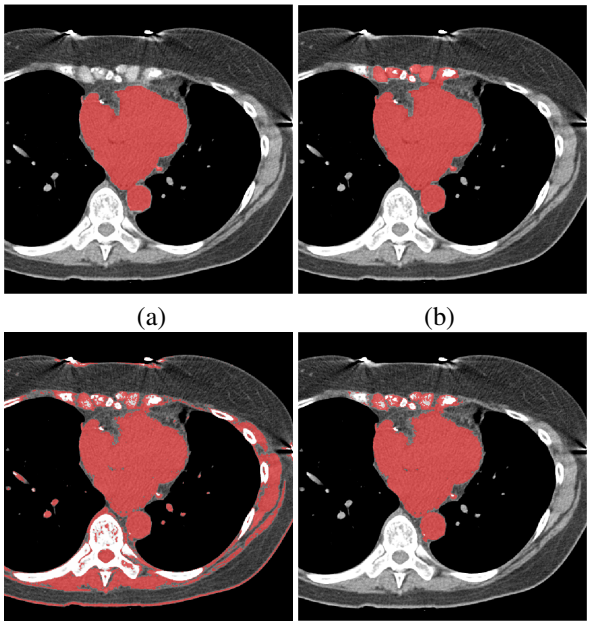

(a) (b) (c) (d)

Figure 6. A comparison of segmentation results obtained using different methods. (a) Fuzzy-Cuts, (b) Fuzzy-Cuts using fuzzy connectivity prior only, (c) BGC (Sec. 3.6 (b)), (d) RFC (Sec. 3.6 (c)).

(b) **Fuzzy-Cuts vs Graph-Cuts**
Figures 6(a) and (c) depict a comparison of Fuzzy-Cuts against the graph-cuts-based method proposed by Boykov *et al.* [4] (BGC). Since their method uses only intensity-likelihood information to define the t-link weights, all the pixels that have an appearance similar to the seed region of the foreground were labeled as foreground irrespective of whether or not they actually belong to the foreground.

(c) **Fuzzy-Cuts vs Relative Fuzzy Connectedness**
Figures 6(a) and (d) depict a comparison of Fuzzy-Cuts against simple, non-iterative, relative fuzzy connectedness proposed by Udupa *et al.* [18] (RFC). In relative fuzzy connectedness, a pixel is assigned to an object that has the strongest affinity path to it in comparison to all the other objects. Since the affinity is a function of appearance only, the segmentation leaks out into neighboring organs with similar appearance as the foreground.

We applied Fuzzy-Cuts to segment the heart in the origin of aorta slice (see Figure 1) of non-contrast cardiac CT scans from 30 patients. The accuracy of the segmentation results obtained were evaluated by measuring the degree of overlap with manual segmentation performed by an expert. The degree of overlap was estimated using the Dice similarity coefficient (DSC). Table 1 provides descriptive statistics of the DSC measure obtained by Fuzzy-cuts in comparison with other methods discussed above.

Table 1. Descriptive statistics of the Dice similarity coefficient (DSC) obtained by Fuzzy-Cuts in comparison with BGC (Sec. 3.6 (b)), and RFC (Sec. 3.6 (c)).

	DSC ($mean \pm std$)	DSC Range
Fuzzy-Cuts	0.88 ± 0.03	[0.78, 0.95]
RFC	0.79 ± 0.10	[0.60, 0.95]
BGC	0.59 ± 0.08	[0.44, 0.76]

4. Conclusion

In this paper, we have presented Fuzzy-Cuts, a novel, knowledge-driven, graph-based method for medical image segmentation. Fuzzy-Cuts introduces a new fuzzy theoretic approach to incorporate knowledge-driven constraints into the MAP-MRF formulation of the segmentation problem. It combines the strengths of both fuzzy and probabilistic approaches into an elegant segmentation framework. Fuzzy-Cuts currently incorporates prior information about an object's location, appearance, and spatial connectivity to a known seed region. In general, any prior that can be represented as a spatial fuzzy set can be readily incorporated into the proposed framework. The incorporation of additional prior information (e.g., shape) will be a topic of our future research.

5. Acknowledgments

This work was supported in part by NSF Grants IIS-0431144, and CNS-0521527 and the UH Eckhard Pfeiffer Endowment Fund.

References

[1] I. Bloch. Fuzzy spatial relationships for image processing and interpretation: a review. *Image and Vision Computing*, 23(2):89–110, 2005.

[2] Y. Boykov and G. Funka-Lea. Graph cuts and efficient N-D image segmentation. *International Journal of Computer Vision*, 70(2):109–131, 2006.

[3] Y. Boykov, O. Veksler, and R. Zabih. Fast approximate energy minimization via graph cuts. *IEEE Trans. on Pattern Analysis and Machine Intelligence*, 23(11):1222–1239, 2001.

[4] Y. Y. Boykov and M. P. Jolly. Interactive graph cuts for optimal boundary and region segmentation of objects in n-D images. In *Proc.* 8^{th} *IEEE International Conference on Computer Vision*, volume 1, pages 105–112, 2001.

[5] O. Camara, O. Colliot, and I. Bloch. Computational modeling of thoracic and abdominal anatomy using spatial relationships for image segmentation. *Real-Time Imaging*, 10(4):263–273, 2004.

[6] T. Chen and D. Metaxas. A hybrid framework for 3D medical image segmentation. *Medical Image Analysis*, 9(6):547–565, 2005.

[7] D. M. Greig, B. T. Porteous, and A. H. Seheult. Exact maximum a posteriori estimation for binary images. *Journal of the Royal Statistical Society. Series B (Methodological)*, 51(2):271–279, 1989.

[8] J. M. Hammersley and P. Clifford. Markov field on finite graphs and lattices, 1971.

[9] P. Kohli and P. Torr. Efficiently solving dynamic Markov random fields using graph cuts. In *Proc.* 10^{th} *IEEE International Conference on Computer Vision*, volume 2, pages 922–929, 2005.

[10] V. Kolmogorov and R. Zabin. What energy functions can be minimized via graph cuts? *IEEE Trans. on Pattern Analysis and Machine Intelligence*, 26(2):147–159, 2004.

[11] U. Kurkure. *Computational methods for non-invasive cardiovascular image analysis*. PhD thesis, University of Houston, Houston, TX, May 2008.

[12] S. Z. Li. *Markov random field modeling in computer vision*. Springer-Verlag, 1995.

[13] R. P. Nikhil and K. P. Sankar. A review on image segmentation techniques. *Pattern Recognition*, 26(9):1277–1294, 1993.

[14] H. Park, P. Bland, and C. Meyer. Construction of an abdominal probabilistic atlas and its application in segmentation. *IEEE Trans. on Medical Imaging*, 22(4):483–92, 2003.

[15] A. S. Pednekar and I. A. Kakadiaris. Image segmentation based on fuzzy connectedness using dynamic weights. *IEEE Trans. on Image Processing*, 15(6):1555–1562, 2006.

[16] D. L. Pham, C. Xu, and J. L. Prince. Current methods in medical image segmentation. *Annual Review of Biomedical Engineering*, 2:315–37, 2000.

[17] M. Sonka, V. Hlavac, and R. Boyle. *Image processing, analysis, and machine vision: third edition*. Thomson, 2008.

[18] J. K. Udupa, P. K. Saha, and R. A. Lotufo. Relative fuzzy connectedness and object definition: theory, algorithms, and applications in image segmentation. *IEEE Trans. on Pattern Analysis and Machine Intelligence*, 24(11):I–1500, 2002.

[19] J. K. Udupa and S. Samarasekera. Fuzzy connectedness and object definition: Theory, algorithms, and applications in image segmentation. *Graphical Models and Image Processing*, 58(3):246–261, 1996.